Metal−1,4-Dithio-2,3-dihydroxybutane Chelates: Novel Inhibitors of the Rho Transcription Termination Factor†

Thomas P. Weber,‡ William R. Widger,§ and Harold Kohn*,||

Department of Chemistry, University of Houston, Houston, Texas 77204-5641, Department of Biology and Biochemistry, University of Houston, Houston, Texas 77204-5934, and Division of Medicinal Chemistry and Natural Products, School of Pharmacy, University of North Carolina, Chapel Hill, North Carolina 27599-7360

Received April 14, 2003; Revised Manuscript Received May 19, 2003

ABSTRACT: Rho is an enzyme that is essential for the growth and survival of *Escherichia coli*, and bicyclomycin (**1**) is its only known selective inhibitor. We show that metal (Cd^{2+}, Ni^{2+}, and Zn^{2+}) complexes of 1,4-dithio-2,3-dihydroxybutanes (**2**) serve as effective and potent rho inhibitors with I_{50} values that can exceed that of **1**. Maximal inhibition for $ZnCl_2$ and L-dithiothreitol (**2a**) corresponded to Zn_2:L-DTT stoichiometry. The I_{50} value for the 2:1 Zn−L-DTT solution was 20 μM, which made it 3 times more potent than **1** (I_{50} = 60 μM). Kinetic studies showed that a Zn−L-DTT solution functioned as a noncompetitive inhibitor with respect to ATP in the rho poly(C)-dependent ATPase assay and as a competitive inhibitor with respect to ribo$(C)_{10}$ in the poly(dC)·ribo$(C)_{10}$-stimulated ATPase assay. These findings demonstrated that both **1** and a Zn−L-DTT solution disrupted rho-mediated ATP hydrolysis but that they inhibit using different mechanisms. Substitution of L-DTT with 1,2-ethanedithiol in $ZnCl_2$ solutions led to a comparable loss of rho poly(C)-dependent ATPase activity, indicating that other metal chelates can serve as efficient inhibitors. The site and pathway of rho inhibition by the putative metal−1,4-dithio-2,3-dihydroxybutane chelates are discussed in light of the current data.

Rho-dependent transcription termination is a regulatory process that controls the expression of genes in most prokaryotes (*1*). In *Escherichia coli*, select termination events require the presence of rho (*2*), and the disruption of rho function leads to the loss of cellular viability.

Rho is a hexamer of 47 kDa identical subunits arranged in a toroidal shape (*2*) with either *C*6/*C*3 symmetry (*3*) or *C*6 symmetry in the absence of ATP (*4*). Mechanistic investigations support a "tethered-tracking" pathway for rho function (*2*) in which rho binds to specific RNA sequences and then translocates (5′ → 3′) along the nascent RNA, using binding sites located within the central hole in a process fueled by Mg^{2+}-mediated ATP hydrolysis (*5*). Transcript termination results when rho encounters the stalled RNA polymerase.

Rho is unique to most prokaryotic bacteria and thus is an attractive macromolecular target for drug intervention. The only reported selective inhibitor of rho is the natural product and commercial agent bicyclomycin (**1**) (*6*). We have demonstrated that **1** both interferes with rho RNA tracking and disrupts ATP hydrolysis (*7*, *8*). In 1964, Cleland showed that dithiothreitol (DTT,[1] **2a**) and its isomer dithioerythreitol (DTE, **2b**) quantitatively converted disulfides to their corresponding thiols (*9*). These 1,4-dithio-2,3-dihydroxybutanes (DTX, **2**) have become the reagents of choice for protecting sulfhydryl groups in enzymes. Here, we report that select metal−DTX species inhibit rho by a unique pathway and that these agents can surpass **1** in potency.

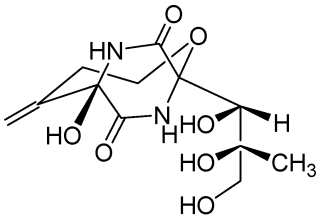

1

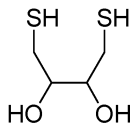

2a DTT
b DTE

MATERIALS AND METHODS

Materials. Bicyclomycin was provided as a gift from Fujisawa Pharmaceutical Co., Ltd. (Osaka, Japan), and was purified by three successive silica gel chromatographies using a 20% methanol/chloroform solution as the eluant. [γ-^{32}P]-ATP (6000 Ci/mmol) was purchased from Perkin-Elmer (Boston, MA); Bio-Spin 6 columns were from Bio-Rad (Hercules, CA), and PEI-TLC plates used for ATPase assays were obtained from J. T. Baker, Inc. (Phillipsburg, NJ). Poly(C) was from Sigma (St. Louis, MO) and was dissolved in 100 μL of TE buffer and dialyzed against aqueous 1.0 M

† This work was supported by National Institutes of Health Grant GM37934 and Robert A. Welch Foundation Grant E1381 (W.R.W.).

* To whom correspondence should be addressed. E-mail: harold_kohn@unc.edu.

‡ Department of Chemistry, University of Houston.

§ Department of Biology and Biochemistry, University of Houston.

|| University of North Carolina.

[1] Abbreviations: DTE, dithioerythreitol; DTT, dithiothreitol; DTX, 1,4-dithio-2,3-dihydroxybutanes; EDTA, ethylenediaminetetraacetic acid; PEI-TLC, poly(ethylenimine) thin-layer chromatography; SDS−PAGE, sodium dodecyl sulfate−polyacrylamide gel electrophoresis; TE, Tris-HCl and EDTA; Tris, tris(hydroxymethyl)aminomethane.

10.1021/bi030089w CCC: $25.00
Published on Web 07/09/2003

potassium phosphate (pH 7.0, 8 h, twice, 4 °C) using Slide-A-Lyzer cassettes from Pierce (Rockford, IL). All other chemicals were reagent grade.

Bacterial Strains and Plasmids. Wild-type rho from *E. coli* was purified as described by Mott (*10*) from strain AR120 containing plasmid p39-ASE (*11*). Rho purity was determined by SDS−PAGE, and protein concentrations were measured according to the Lowry assay (*12*).

Rho Poly(C)-Dependent ATPase Assay (13). The ribonucleotide-stimulated ATPase activity of rho at 32 °C was assayed by the amount of ^{32}P-labeled inorganic phosphate hydrolyzed from ATP after separation on PEI-TLC plates (prerun with water and dried) using 0.75 M potassium phosphate (pH 3.5) as the mobile phase. Reactions were initiated by adding ATP (varying concentrations) and 0.5 μCi of [γ-^{32}P]ATP to the solution containing 40 mM Tris-HCl (pH 7.9), 50 mM KCl, 100 or 250 nM poly(C), 100 or 250 nM rho (monomer), and $MgCl_2$ (1 or 10 mM). The TLC plates were exposed to PhosphorImager plates (Fuji and Molecular Dynamics) (3 h), scanned on a Storm 860 PC PhosphorImager, and analyzed using ImageQuant version 5.0 from Molecular Dynamics. The initial rates of the reactions were determined by plotting the amount of ATP hydrolyzed against time. Each reaction was performed in duplicate, and the results were averaged.

Inhibition of Rho Poly(C)-Dependent ATPase Activity by Metal−D,L-DTT Chelates. ATPase assays were carried out as described in the preceding section using a six-channel, multiwell procedure (*14*). The reactions (100 μL) were run with 250 μM ATP in the presence of the metal−DL-DTT (1:1) solution (0−500 μM) and 1 mM $MgCl_2$. Samples were preincubated at 32 °C for 2 min, and then ATP was added. Five 1.4 μL aliquots were spotted onto PEI-TLC plates after 15 s and then at selected times (10−300 s) thereafter. Plates were analyzed as described previously. Each reaction was performed in duplicate, and the results were averaged.

Inhibition of Rho Poly(C)-Dependent ATPase Activity by the Zn−L-DTT Chelate. Stoichiometry of the Inhibitor. The poly(C)-dependent ATPase assays were carried out as described in the preceding section using an eight-channel, multiwell procedure (*14*). The duplicated reactions (100 μL) were run with 250 μM ATP and 10 mM $MgCl_2$ in the presence of 0, 2.5, 5, 10, 20, 40, 80, 160, and 320 μM $ZnCl_2$. Each of the preceding experiments was then repeated in the presence of 0, 2.5, 5, 10, 20, 40, 80, 160, and 320 μM L-DTT, resulting in a 9 × 9 reaction matrix. Samples were preincubated at 32 °C for 2 min prior to ATP addition, and five 1.4 μL aliquots were spotted onto PEI-TLC plates every 15 s. The plates were treated as described previously. The data were analyzed using SigmaPlot 2001 using the XYZ triplet line plot function and plotted as a color-coded, three-dimensional mesh and contour plot (Figure 2A). The fractional inhibition (0.1, 0.2, ..., 0.9) in the contour plots was determined from the inhibition curves. Concentration combinations of Zn^{2+} and L-DTT that gave equal fractional inhibition were plotted (Figure 2B).

Kinetics of Rho Poly(C)-Dependent ATPase Activity and Inhibition by the Zn−L-DTT Solution (1:1). ATPase assays were carried out as described in the preceding section using a six-channel, multiwell procedure (*14*). The reactions (100 μL) were run with 2.5, 5, 10, 20, 40, 80, 160, 320, and 640 μM ATP in the presence of 10 mM $MgCl_2$. Each series was repeated in the presence of 10, 20, 40, 80, or 160 μM Zn−L-DTT solution (1:1). Samples were preincubated at 32 °C for 2 min prior to ATP addition, and five 1.4 μL aliquots were spotted onto PEI-TLC plates after 15 s and then at selected times (10−300 s), depending upon the ATP concentrations. Plates were analyzed as described previously. Each reaction was performed in duplicate, and the results were averaged.

Rho Poly(dC)·Ribo(C)$_{10}$-Dependent ATPase Assay (15). The ribonucleotide-stimulated ATPase activity of rho at 32 °C was assayed by the amount of ^{32}P-labeled inorganic phosphate hydrolyzed from ATP after separation on PEI-TLC plates (prerun with water and dried) using 0.75 M potassium phosphate (pH 3.5) as the mobile phase. Reactions were initiated by adding 200 μM ATP and 0.5 μCi of [γ-^{32}P]-ATP to the solution containing 40 mM Tris-HCl (pH 7.9), 50 mM KCl, 200 nM poly(dC), 100 nM rho (monomer), ribo(C)$_{10}$ (various concentrations), and 10 mM $MgCl_2$, and five 1.4 μL aliquots were spotted onto PEI-TLC plates every 15 s. Plates were analyzed as described previously. Each reaction was performed in duplicate, and the results were averaged.

Kinetics of Rho Poly(dC)·Ribo(C)$_{10}$-Stimulated ATPase Activity and Inhibition by the Zn−L-DTT Solution (1:1). ATPase assays were carried out as described in the preceding section using a six-channel, multiwell procedure (*14*). The reactions (30 μL) were run with 0.75, 1.5, 3, 6, 12, 24, 48, and 96 μM ribo(C)$_{10}$. Each series was repeated in the presence of 10, 20, 40, and 80 μM Zn−L-DTT chelate. Samples were preincubated at 32 °C for 2 min prior to ATP addition, and five 1.4 μL aliquots were spotted onto PEI-TLC plates after 15 s and then at selected times (10−300 s) thereafter. Plates were analyzed as described previously. Each reaction was performed in duplicate, and the results were averaged.

Promiscuity Tests for the Zn−L-DTT Solution (1:1) and Bicyclomycin. The rho poly(C)-dependent ATPase activity measurements were conducted using a solution (100 μL) containing rho [100 nM (monomer)], poly(C) (100 nM), ATP (200 μM), $MgCl_2$ (10 mM), and either Zn−L-DTT solution (1:1) (0−800 μM) or **1** (0−400 μM) at 32 °C for a 2 min preincubation. The average velocities of two determinations are plotted. Each of the preceding experiments was then repeated as follows: the preincubation times were varied, the rho and poly(C) concentrations were increased to 1 μM, and the reaction mixture contained 0.1 mg/mL BSA. The reactions were analyzed as described above.

Inhibition of Rho Poly(C)-Dependent ATPase Activity by Zn Chelates. The poly(C)-dependent ATPase assays were carried out as described in the preceding section using a six-channel, multiwell procedure (*14*). The reactions (100 μL) were run with 200 μM ATP in the presence of 0, 25, 50, 100, 200, and 400 μM Zn solution (1:1) (Zn−2-mercaptoethanol or Zn−1,2-ethanedithiol). Samples were preincubated at 32 °C for 2 min prior to ATP addition, and five 1.4 μL aliquots were spotted onto PEI-TLC plates every 15 s. Plates were analyzed as described previously. Each reaction was performed in duplicate, and the results were averaged.

RESULTS

$CdCl_2$, $MnCl_2$, $NiCl_2$, and $ZnCl_2$ in DL-DTT-free buffer solutions all activated rho poly(C)-dependent ATP hydrolysis

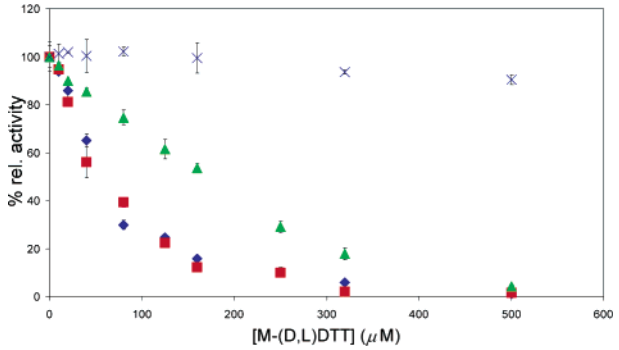

FIGURE 1: Metal−DL-DTT (1:1) inhibition of rho poly(C)-dependent ATPase activity. The reactions were conducted using a 100 μL solution containing ATPase buffer, rho [250 nM (monomer)], poly(C) (250 nM), ATP (200 μM), $MgCl_2$ (1 mM), and the metal−DL-DTT solution (1:1) (0−500 μM) at 32 °C. The average velocities of two determinations are plotted: Zn−DL-DTT (diamonds), Cd−DL-DTT (squares), Ni−DL-DTT (triangles), and Mn−DL-DTT (times signs).

in the absence of $MgCl_2$ (*14*). Surprisingly, after adding an equimolar amount of DL-DTT to solutions containing either $CdCl_2$, $NiCl_2$, or $ZnCl_2$ in the presence of $MgCl_2$ (1 mM), we saw a pronounced loss of rho activity (I_{50}): 60 μM for $CdCl_2$, 160 μM for $NiCl_2$, and 55 μM for $ZnCl_2$ (Figure 1).[2] However, DL-DTT (0.1−0.3 mM) alone or in combination with either $MnCl_2$ (Figure 1) or $MgCl_2$ did not inactivate the enzyme. Thus, we concluded that the DTT-mediated inactivation process was metal specific.

We focused our studies on $ZnCl_2$ with DTX and defined the parameters that governed metal chelate inhibition of rho poly(C)-dependent ATPase activity. Data were obtained after preincubating (2 min at 32 °C) the inhibitor, rho, and poly(C) in the buffer solution prior to adding ATP to initiate the assay. First, we examined the effect of DTX stereochemistry on rho poly(C)-dependent ATPase inhibition. The three stereoisomers for DTX are D-DTT, L-DTT, and the *meso* form, dithioerythritol (DTE). L-DTT, DL-DTT, and DTE are commercially available. Slight differences in the I_{50} values were observed for the 1:1 $ZnCl_2$−DTX solutions (0−800 μM) as we varied the chelator (I_{50} values, 60 μM for Zn−DL-DTT, 50 μM for Zn−L-DTT, and 60 μM for Zn−DTE; data not shown) in the presence of 10 mM $MgCl_2$. This finding indicates that the inhibitor−protein interaction was independent of the DTX configuration. Next, we determined the $ZnCl_2$:DTT stoichiometry for maximal inhibition. DTT has been reported to give metal complexes with different stoichiometries depending on the metal:DTT ratio and their solution concentrations (*17*). We conducted a 9 × 9 matrix experiment in which both the $ZnCl_2$ and the L-DTT concentrations ranged from 0 to 320 μM (Figure 2A). The data showed that maximal inhibition (decreased rho activity) occurred when the $ZnCl_2$:L-DTT ratio was 2:1 (Figure 2B, red line) and that inhibitory activity diminished as the $ZnCl_2$:L-DTT ratio approached 1:2 (Figure 2B, blue and green lines). The I_{50} value for the 2:1 Zn−L-DTT solution was 20 μM, which was 3 times more potent than **1** (I_{50} = 60 μM) (*6*, *18*).

We then investigated the mechanism of Zn−L-DTT (1:1) inhibition of rho ATP hydrolysis with respect to both ATP and ribo$(C)_{10}$. Figure 3A shows the double-reciprocal plot of 1/*V* versus 1/[ATP] at various Zn−L-DTT (1:1) concentrations in the poly(C)-dependent ATP hydrolysis assay (10 mM $MgCl_2$). The graph indicates that the Zn−L-DTT (1:1) solution inhibited the conversion of ATP to ADP and P_i by a noncompetitive pathway, with respect to ATP. When the intercepts and slopes of the double-reciprocal graphs were plotted against the Zn−L-DTT (1:1) concentrations, we obtained straight lines (Figure 3A, inset), suggesting that the inhibitor bound at a unique, noninteracting site with a K_i of 60 μM. A similar kinetic finding has been reported for **1** (K_i = 20 μM) (*18*). Figure 3B depicts the inhibition kinetics for Zn−L-DTT (1:1) solutions in the poly(dC)·ribo$(C)_{10}$-stimulated ATPase assay (10 mM $MgCl_2$). We found that the Zn−L-DTT (1:1) solution was a competitive inhibitor with respect to ribo$(C)_{10}$. This finding differed from **1**, which showed a mixed inhibition pattern (*7*). The K_M for ribo$(C)_{10}$ was measured as 4 μM in the absence of inhibitor and increased to 20 μM at 80 μM Zn−L-DTT chelate. For the Zn−L-DTT (1:1) solution, we observed a K_i of 28 μM (Figure 3B, inset). Thus, **1** and Zn−L-DTT solution (1:1) both disrupted rho-mediated ATP hydrolysis, but they functioned by different pathways.

With the use of high-throughput and virtual screening techniques, the number of new lead compounds for drug development has dramatically increased. The validity of some of these new leads has been questioned (*19*), and attention is now focused on determining the inhibition pathway for these compounds and whether the inhibitors exhibit enzyme specificity. Compounds that exhibit nonspecific interaction have been defined as "promiscuous inhibitors". We tested the inhibitor specificity of Zn−L-DTT complexes. The I_{50} (30 μM) value for Zn−L-DTT (1:1) solutions was not affected appreciably either by adding BSA (0.1 mg/mL) (I_{50} = 40 μM) or by a 10-fold increase in rho concentration (I_{50} = 60 μM) (Figure 4) (*19*). Next, we examined the time dependency for chelate inhibition since a well-behaved, reversible inhibitor is typically not affected by incubation time (*19*). Maximal inhibition was observed for the Zn−L-DTT chelate after preincubation of the reaction mixture, without ATP, for 2 min. Without preincubation, no loss of rho activity was observed (Figures 4 and 5). When we tested **1** in a similar way, we found that its I_{50} value (50 μM) was not significantly affected when BSA (0.1 mg/mL) was included, when the rho concentration was increased (10-fold), or when the inhibitor preincubation time was reduced to zero (Figure 6). We then asked whether Zn−L-DTT (1:1) solutions inhibited *E. coli* RecA poly(dT)-dependent ATPase activity (*20*, *21*). Recent electron micrograph studies of rho and RecA show that the cores of these proteins are structurally similar (*22* and references therein). $ZnCl_2$ (125 μM) led to modest reductions (0−30%) in the ATP hydrolysis rate for the poly(dT) concentrations (0−25 μM) that were tested (data not shown). Addition of an equimolar amount of L-DTT to the $ZnCl_2$ solution did not cause further reductions in the rate, indicating that Zn−L-DTT complexes did not inhibit RecA poly(dT)-dependent ATP hydrolysis. Similarly, no loss of RecA ATPase activity was observed when **1** (0−400 μM) was included in the reaction solution. These collective findings indicate that both the Zn−L-DTT complex and **1** were selective, nonpromiscuous inhibitors and that binding of the Zn−L-DTT solution (1:1) to rho was slow or the

[2] An earlier study reported that $CdCl_2$ and $ZnCl_2$ rho solutions maintained in buffer solutions containing DL-DTT inhibited rho and that the inhibitory species was the divalent metal; see ref *16*.

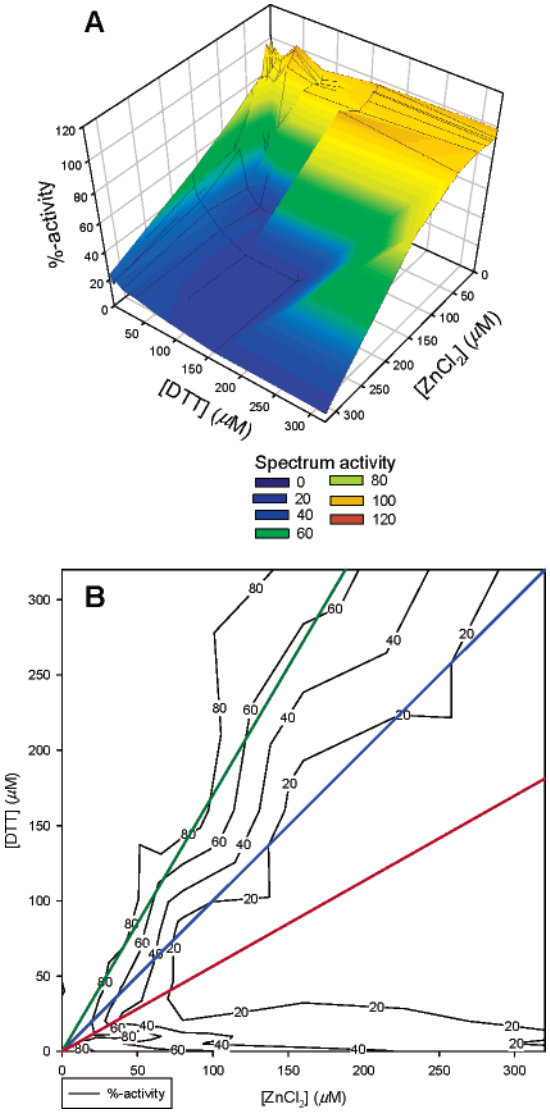

FIGURE 2: (A) Zn−L-DTT inhibition of rho poly(C)-dependent ATPase activity as a function of $ZnCl_2$ and L-DTT concentration. The reactions were conducted using a 100 μL solution containing ATPase buffer, rho [200 nM (monomer)], poly(C) (200 nM), ATP (200 μM), $MgCl_2$ (10 mM), and combinations of $ZnCl_2$ (0−320 μM) and L-DTT (0−320 μM) at 32 °C. The average normalized velocities (*z*-axis) of two determinations are plotted as a function of total $ZnCl_2$ (*y*-axis) and total L-DTT concentration (*x*-axis). (B) Zn−L-DTT inhibition isobals. The isobals (20, 40, ..., 100%) give the degree of enzyme activity. The green, blue, and red lines correspond to 1:2, 1:1, and 2:1 $ZnCl_2$−L-DTT solutions, respectively.

chelating species underwent structural reorganization prior to binding.

We have made several attempts to determine if the Zn−L-DTT solution (1:1) inhibited bacterial growth. Using W3350 *E. coli* and either a filter disk (*23*) or a liquid culture (*24*) assay, we observed the apparent precipitation of the inhibitor with no loss of bacterial growth when the Zn−L-DTT solution (1:1) was added to the medium.

Next, we asked whether $ZnCl_2$ solutions containing either 1,2-ethanedithiol or 2-mercaptoethanol inhibited rho poly-(C)-dependent ATPase activity and compared the results to those with L-DTT. The I_{50} value for $ZnCl_2$ solutions containing equimolar amounts of either L-DTT, 1,2-ethanedithiol, or 2-mercaptoethanol in the presence of 10 mM $MgCl_2$ was 45, 50, or 175 μM, respectively (Figure 7).

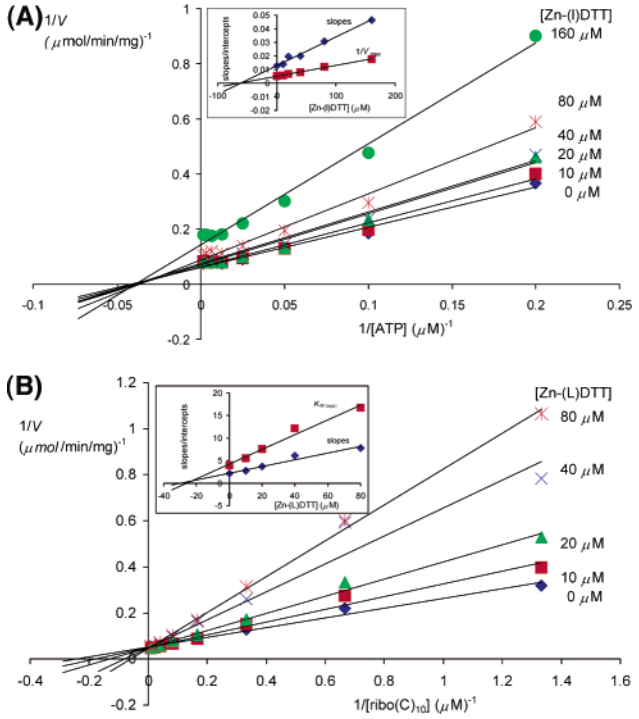

FIGURE 3: (A) Zn−L-DTT inhibition of rho in the poly(C)-dependent ATPase assay. The double-reciprocal plot of rho poly-(C)-dependent ATPase activity vs ATP concentrations for varying concentrations of the Zn−L-DTT solution (1:1). Values are the averages of duplicate reactions. The inset shows a plot of the slopes (diamonds) and intercepts (squares) vs Zn−L-DTT concentration. (B) Zn−L-DTT inhibition of rho in the poly(dC)·ribo$(C)_{10}$-dependent ATPase assay. The double-reciprocal plot of the poly-(dC)·ribo$(C)_{10}$-dependent ATPase activity of rho with varying concentrations of the Zn−L-DTT solution (1:1). Values are the averages of duplicate reactions. The inset shows a plot of the slopes (diamonds) and intercepts (squares) vs Zn−L-DTT concentration.

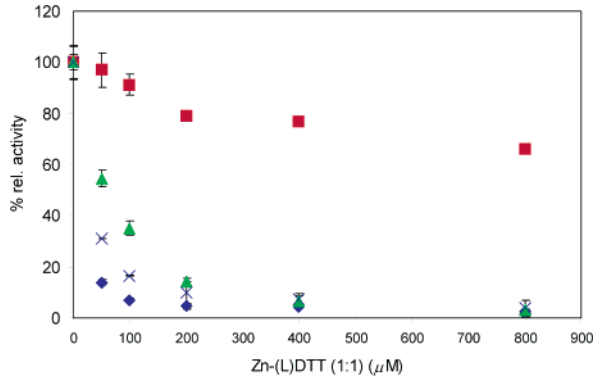

FIGURE 4: Promiscuity test for the Zn−L-DTT chelate. The reactions were conducted using a 100 μL solution containing rho [100 nM (monomer)], poly(C) (100 nM), ATP (200 μM), $MgCl_2$ (10 mM), and Zn−L-DTT (0−800 μM) at 32 °C. The average velocities of two determinations are plotted for the control (diamonds), no preincubation (squares), a 10-fold concentration of rho, poly(C), and ATP (triangles), and the standard condition with 0.1 mg/mL BSA (times signs).

Thus, we tentatively concluded that Zn−dithiol chelates were more effective than Zn−mercaptoalkanol adducts in inhibiting rho.

DISCUSSION

The transcription termination factor rho is an essential protein necessary for Gram-negative bacterial growth (*1*).

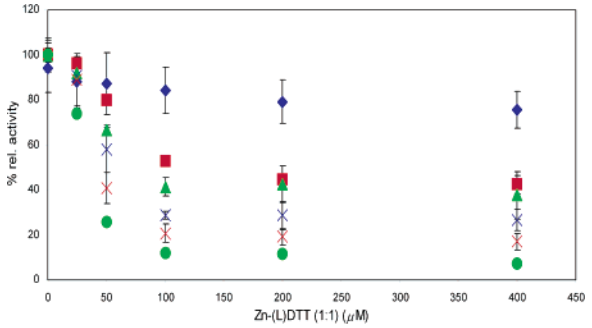

FIGURE 5: Effect of preincubation time on Zn−L-DTT inhibition. The reactions were conducted using a 100 μL solution containing rho [100 nM (monomer)], poly(C) (100 nM), ATP (200 μM), $MgCl_2$ (10 mM), and the Zn−L-DTT complex (0−400 μM) at 32 °C. The average velocities of two determinations are plotted for no preincubation (diamonds), preincubation for 15 s (squares), preincubation for 30 s (triangles), preincubation for 1 min (blue times signs), preincubation for 2 min (red times signs), and preincubation for 5 min (circles).

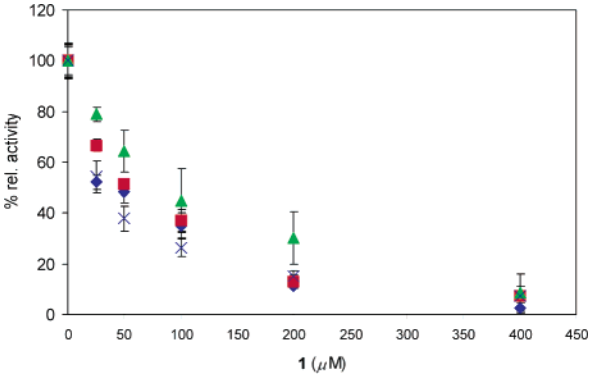

FIGURE 6: Promiscuity test for bicyclomycin. The reactions were conducted using a 100 μL solution containing rho [100 nM (monomer)], poly(C) (100 nM), ATP (200 μM), $MgCl_2$ (10 mM), and **1** (0−400 μM) at 32 °C. The average velocities of two determinations are plotted for the control (diamonds), no preincubation (squares), a 10-fold concentration of rho, poly(C), and ATP (triangles), and the standard condition with 0.1 mg/mL BSA (times signs).

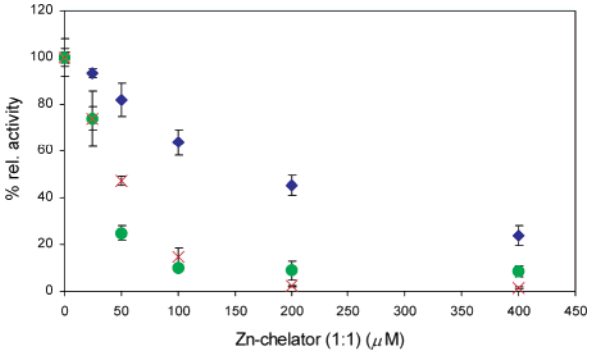

FIGURE 7: Structure−activity relationship for a series of Zn^{2+} chelator solutions (1:1). The reactions were conducted using a 100 μL solution containing rho [100 nM (monomer)], poly(C) (100 nM), ATP (200 μM), $MgCl_2$ (10 mM), and the Zn chelate (0−400 μM) at 32 °C. The average velocities of two determinations are plotted for Zn−2-mercaptoethanol (diamonds), Zn−1,2-ethanedithiol (times signs), and Zn−L-DTT (circles).

Despite the rho protein's central importance in the cell biology of these organisms, the only reported selective inhibitor for this enzyme is the natural product, bicyclomycin (**1**) (*6*). In this study, we document that select metal chelates inhibit rho function by a unique pathway and that the inhibitory activities of these chelates can exceed that of **1**.

Equimolar DL-DTT solutions containing either $ZnCl_2$, $CdCl_2$, or $NiCl_2$ inhibited rho poly(C)-dependent ATP hydrolysis in the presence of $MgCl_2$. Significantly, these metals stimulated rho ATPase activity in the absence of $MgCl_2$ and DL-DTT (*14*). By comparison, DL-DTT (0.1−0.3 mM) by itself or in combination with either $MgCl_2$ (data not shown) or $MnCl_2$ (Figure 1) did not inactivate the enzyme. We observed rho inhibition only when the metal and chelator were both present.

We examined the $ZnCl_2$−L-DTT inhibition and first focused on the structure of the inhibitory complex. The rho poly(C)-dependent inhibitory activities of equimolar solutions of $ZnCl_2$ and either L-DTT (I_{50} = 45 μM) or ethanedithiol (I_{50} = 50 μM) were comparable and were significantly higher than that of an equimolar solution of $ZnCl_2$ and 2-mercaptoethanol (I_{50} = 175 μM), suggesting that binding of metal to DTT preferentially occurred through sulfur rather than oxygen (Figure 7). We found slight differences in the extent of rho inhibition for the Zn chelates of DTT (**2a**) and DTE (**2b**) (data not shown), documenting that the stereochemical disposition of the hydroxy groups did not affect rho inhibition. The stoichiometry for maximal rho poly(C)-dependent ATPase inhibition corresponded to the Zn_2−L-DTT chelate (Figure 2). This stoichiometry differed from those of the previously identified Zn−DL-DTT, Zn−(DL-DTT)$_2$, and Zn_3−(DL-DTT)$_4$ complexes (*17*). Thus, we suspect that the structure of the Zn−DL-DTT rho inhibitory species is affected by protein binding. Indeed, we observed that chelate inhibition required a 2 min preincubation period at 32 °C (Figure 5). Although slow binding inhibitory processes may proceed through changes in protein conformation, the preincubation of 2 min was sufficient to obtain kinetic data that followed a linear response when plotting the slope and intercepts from the double-reciprocal plots (Figure 3A). Moreover, after the 2 min preincubation we did not observe further slowing of the velocity curves, suggesting that steady state rates were being reached within 2 min. We expect that additional details of the inactivation process can be obtained from further study of the time course for inhibition.

The mechanism of Zn−L-DTT inhibition of rho was investigated. The Zn−L-DTT solution (1:1) exhibited noncompetitive kinetics with respect to ATP in the poly(C)-dependent ATPase assay (Figure 3A) and fully competitive kinetics with respect to ribo$(C)_{10}$ in the poly(dC)·ribo$(C)_{10}$ ATPase assay (Figure 3B). These results indicated that the site of Zn−L-DTT inhibition is close to or at the rho secondary RNA binding site (*5*, *25*). The kinetic patterns for the Zn−L-DTT complex differentiated this inhibitor from **1** where reversible, noncompetitive inhibition was observed with respect to ATP in the poly(C)-dependent ATPase assay (*18*), but mixed inhibition was observed with respect to ribo$(C)_{10}$ in the poly(dC)·ribo$(C)_{10}$ ATPase assay (*7*). Thus, while the two inhibitors disrupt ATP hydrolysis, they function by different pathways.

Significantly, the stoichiometry of the inhibitory species alone does not reveal the structure of the complex. Nonetheless, an important inference from our stoichiometric inhibition studies is that the Zn^{2+} likely interacts directly with the protein (*26*) since Zn:DTT ratios of 1:1 or higher are required for rho inhibition. These stoichiometries increase the likeli-

hood that metal coordination sites are formally accessible for binding to rho and permit us to speculate about the Zn_2−L-DTT binding site in rho. Inspection of the rho model showed that histidines line the rho RNA tracking site (*5*). Specific complexation of the Zn_2−L-DTT chelate at one of these sites is consistent with the full competitive inhibition kinetics for Zn−L-DTT solutions obtained with respect to ribo$(C)_{10}$ in the poly(dC)·ribo$(C)_{10}$ ATPase assay (Figure 3B).

CONCLUSIONS

Our studies have documented the potent inhibitory activity of Cd^{2+}−, Ni^{2+}−, and Zn^{2+}−DTT chelates and provide the basis for a new class of site specific rho inhibitors. While we have focused on chelates that consist of Zn^{2+} and thiols, we predict that the different coordination properties of metals and the manifold structural properties of sulfur, oxygen, and nitrogen ligands (*27*) will lead to the discovery of a diverse library of rho inhibitors. Experiments are underway to determine the site of inhibition and the enzyme specificity of these novel inhibitors.

ACKNOWLEDGMENT

This paper is dedicated to Professor Stephen J. Benkovic (The Pennsylvania State University, University Park, PA) on the occasion of his 65th birthday. We thank Dr. Scott Singleton and Mr. Andrew M. Lee (Rice University, Houston, TX) for assessing the inhibitory profile of the Zn−L-DTT solution (1:1) against *E. coli* RecA, Dr. M. Kawamura and the Fujisawa Pharmaceutical Co., Ltd., for the gift of **1**, and Dr. T. Platt (University of Rochester, Rochester, NY) for the overproducing strain of rho.

REFERENCES

1. Yager, T. D., and von Hippel, P. H. (1987) in *The Molecular and Cell Biology of E. coli and S. typhimurium* (Neidhardt, F., Ed.) pp 1241−1275, American Society for Microbiology, Washington, DC.
2. Richardson, J. P. (2002) Rho-dependent termination and ATPases in transcript termination, *Biochim. Biophys. Acta 1577*, 251−260.
3. Vincent, F., Openshaw, M., Trautwein, M., Gaskell, S. J., Kohn, H., and Widger, W. R. (2000) Rho transcription factor: Symmetry and binding of bicyclomycin, *Biochemistry 39*, 9077−9083.
4. Yi, X., Johnson, J., Kohn, H., and Widger, W. R. (2003) ATP binding to rho transcription termination factor. Mutant F355W ATP-induced fluorescence quenching reveals dynamic ATP binding, *J. Biol. Chem. 278*, 13719−13727.
5. Xu, Y., Kohn, H., and Widger, W. R. (2002) Mutations in the rho transcription termination factor that affect RNA tracking, *J. Biol. Chem. 277*, 30023−30030.
6. Zwiefka, A., Kohn, H., and Widger, W. R. (1993) Transcription termination factor rho: The site of bicyclomycin inhibition in *Escherichia coli*, *Biochemistry 32*, 3564−3570.
7. Magyar, A., Zhang, X., Kohn, H., and Widger, W. R. (1996) The antibiotic bicyclomycin affects the secondary RNA binding site of *Escherichia coli* transcription termination factor Rho, *J. Biol. Chem. 271*, 25369−25374.
8. Weber, T. P., Widger, W. R., and Kohn, H. (2002) The Mg^{2+} requirements for rho transcription termination factor: Catalysis and bicyclomycin inhibition, *Biochemistry 41*, 12377−12383.
9. Cleland, W. W. (1964) Dithiothreitol, a new protective group for SH groups, *Biochemistry 3*, 480−482.
10. Mott, J. E., Grant, R. A., Ho, Y.-S., and Platt, T. (1985) Maximizing gene expression from plasmid vectors containing the λ P_L promoter: Strategies for overproducing transcription termination factor ρ, *Proc. Natl. Acad. Sci. U.S.A. 82*, 88−92.
11. Nehrke, K. W., Seifried, S. E., and Platt, T. (1992) Overproduced rho factor from p39AS has lysine replacing glutamic acid at residue 155 in the linker region between its RNA and ATP binding domains, *Nucleic Acids Res. 20*, 6107.
12. Lowry, O. H., Rosebrough, N. J., Farr, A. L., and Randall, R. J. (1951) Protein measurement with the folin phenol reagent, *J. Biol. Chem. 193*, 265−275.
13. Sharp, J. A., Galloway, J. L., and Platt, T. (1983) A kinetic mechanism for the poly(C)-dependent ATPase of the *Escherichia coli* transcription termination protein, rho, *J. Biol. Chem. 258*, 3482−3486.
14. Weber, T. P., Widger, W. R., and Kohn, H. (2003) Metal dependency for transcription factor rho activation, *Biochemistry 42*, 1652−1659.
15. Richardson, J. P. (1982) Activation of rho protein ATPase requires simultaneous interaction at two kinds of nucleic acid-binding sites, *J. Biol. Chem. 257*, 5760−5766.
16. Lowery, C., and Richardson, J. P. (1977) Characterization of the nucleoside triphosphate phosphohydrolase (ATPase) activity of RNA synthesis termination factor ρ. I. Enzymatic properties and effects of inhibitors, *J. Biol. Chem. 252*, 1375−1380.
17. Krezel, A., Lesniak, W., Jezowska-Bojczuk, M., Mlynarz, P., Brasun, J., Kozlowski, H., and Bal, W. (2001) Coordination of heavy metals by dithiothreitol, a commonly used thiol group protectant, *J. Inorg. Biochem. 84*, 77−78.
18. Park, H.-g., Zhang, X., Moon, H.-s., Zwiefka, A., Cox, K., Gaskell, S. J., Widger, W. R., and Kohn, H. (1995) Bicyclomycin and dihydrobicyclomycin inhibition kinetics of *Escherichia coli* rho-dependent transcription termination factor ATPase activity, *Arch. Biochem. Biophys. 323*, 447−454.
19. McGovern, S. L., Caselli, E., Grigorieff, N., and Shoichet, B. K. (2002) A common mechanism underlying promiscuous inhibitors from virtual and high-throughput screening, *J. Med. Chem. 45*, 1712−1722.
20. Morrical, S. W., Lee, J., and Cox, M. M. (1986) Continuous association of *Escherichia coli* single-stranded DNA binding protein with stable complexes of RecA protein and single-stranded DNA, *Biochemistry 25*, 1482−1494.
21. Berger, M. D., Lee, A. M., Simonette, R. A., Jackson, B. E., Roca, A. I., and Singleton, S. (2001) Design and evaluation of tryptophanless RecA protein with wild-type activity, *Biochem. Biophys. Res. Commun. 286*, 1195−1203.
22. Yu, X., Horiguchi, T., Shigesada, K., and Egelman, E. H. (2000) Three-dimensional reconstruction of transcription termination factor rho: Orientation of the N-terminal domain and visualization of an RNA-binding site, *J. Mol. Biol. 299*, 1279−1287.
23. Ericsson, H. M., and Sherris, J. C. (1971) Antibiotic sensitivity testing. Report of an international collaborative study, *Acta Pathol. Microbiol. Scand., Sect. A 217* (Suppl.), 1−90.
24. Kim, M. G., Strych, U., Krause, K., Benedik, M., and Kohn, H. (2003) *N*(2)-Substituted D,L-cycloserine derivatives: Synthesis and evaluation as alanine racemase inhibitors, *J. Antibiot. 56*, 160−168.
25. Wei, R. R., and Richardson, J. P. (2001) Mutational changes of conserved residues in the Q-loop region of transcription factor rho greatly reduce secondary site RNA-binding, *J. Mol. Biol. 314*, 1007−1015.
26. Parkin, G. (2000) The bioinorganic chemistry of zinc enzymes that feature tripodal ligands, *Chem. Commun.*, 1971−1985.
27. Louie, A. Y., and Meade, T. J. (1999) Metal complexes as enzyme inhibitors, *Chem. Rev. 99*, 2711−2734.

BI030089W